Gint4.T modified DNA tetrahedron loaded with doxorubicin inhibits glioma cell proliferation by targeting PDGFRβ

Feng Wang (fengfly1984@163.com)
Chongqing Medical University https://orcid.org/0000-0002-4154-6507
Yanghao Zhou
Chongqing Medical University Second Affiliated Hospital department of neurosurgery
Si Cheng
Chongqing Medical University Second Affiliated Hospital Department of Orthopedics
Jinhe Lou
chongqing general hospital department of neurology
Qiuguang He
Chongqing Medical University second Affiliated Hospital department of neurosurgery
Yuan Cheng
Chongqing Medical University Second Affiliated Hospital, department of neurosurgery

Nano Express

Keywords: glioma, p latelet derived growth factor receptor β , Gint4 T, DNA tetrahedron, nanostructures

Posted Date: February 6th, 2020

DOI: https://doi.org/10.21203/rs.2.22796/v1

Version of Record: A version of this preprint was published on July 20th, 2020. See the published version at https://doi.org/10.1186/s11671-020-03377-y.

Gint4.T modified DNA tetrahedron loaded with doxorubicin inhibits glioma cell proliferation by targeting PDGFRβ

Feng Wang[1], Yanghao Zhou[1], Si Cheng[2], Jinhe Lou[3], Qiuguang He[1], Ning Huang[1], Yuan Cheng[1]*

1.Department of Neurosurgery, the Second Affiliated Hospital of Chongqing Medical University,

2.Department of Orthopedics, the Second Affiliated Hospital of Chongqing Medical University,

3.Department of Neurology, Chongqing General Hospital.

*** Correspondence to**: Yuan Cheng, **Email:** chengyuan023@aliyun.com, **tel:** +86 13708329653

Abstract

Glioma is one of the most deadly tumors due to invasive growth. The treatment effect is poor due to the presence of the blood brain barrier (BBB) and blood tumor barrier (BTB) and insufficient drug targeting. DNA tetrahedron (TDN) is considered to have great potential for drug delivery and maybe a novel therapeutic strategy for glioma. In this study, we have developed a doxorubicin loaded-DNA tetrahedron modified by a Gint4.T aptamer(DOX@Apt-TDN) that could target PDGFRβ for therapy of glioma. The TDN and Apt-TDN were self-assembled by one-step synthesis. The characterization and stability were detected using gel electrophoresis analysis, dynamic light scatting and atomic force microscopy. The cytotoxicity of TDN in vitro was determined by CCK-8 assays. Fluorescence spectrophotometry was used to measure the drug loading capacity. Fluorescence microscopy imaging and flow cytometry were used to survey the cellular uptake. The cell viability, cell cycle and early apoptosis were estimated when the U87MG cells were treated with DOX, DOX@TDN and Dox@Apt-TDN. The rusults showed that a single Apt-TDN could carry 60 doxorubicin molecules. The 3D structure of the DNA tetrahedron remarkedly enhanced drug stability in fetal bovine serum, remaining intact for 7h leastwise. The CCK-8 assay showed that the activity of the U87 cells was not affected after co-cultured with different concentrations(10–500 nM) of TDN for 24 h and 48 h. The aptamer Gint4.T enhanced the targeted uptake of TDN by U87MG cells. Dox-loaded Apt-TDN inhibited cell viability and induced early apoptosis. In conclusion this study establishes that the Gint4.T-modified DNA tetrahedron could target PDGFRβ and provide a novel therapy with promising clinical application for gliomas.

Keyword: glioma, platelet-derived growth factor receptor β, Gint4.T, DNA tetrahedron, nanostructures

Introduction

Glioma is a tumor derived from the neuroepithelial and the most common intracranial malignancy. Nearly 1/3 of all brain tumors are glioma, and approximately 4/5 of

primary malignant brain tumors are glioma [1-4]. Currently, the most effective treatment for glioma is surgical resection and postoperative concurrent chemoradiotherapy, but unfortunately the prognosis for patients remains poor. Traditional chemotherapy for glioma lacks efficient outcomes due to poor tumor targeting and complications due to the presence of the blood brain barrier (BBB) and blood tumor barrier (BTB) and insufficient drug targeting. The BBB is the most important factor that prevents almost all macromolecules (contains drugs, gene, etc.) from delivering to the brain parenchyma and functioning properly. The dosages of drugs that cannot across through the BBB have to be sufficiently high to achieve an effective treatment concentration in the area of interest. However, excess drug can cause severe systemic by-effect and unsought drug cumulation in non-affected tissues. Moreover, existing conventional anti-glioma drugs have insufficient targeting capabilities[3-4]. Because of their size advantage, nanoparticles can cross the BBB and exert an anti-tumor effect. Therefore, we investigated the possibility of using TDN in glioma therapy and enhancing its targeting ability.

Platelet-derived growth factor receptor β (PDGFRβ) is an important member of the tyrosine protein kinase family and is involved in cellular proliferation, migration, and angiogenesis. Several studies have shown that PDGF is a promising target for anti-tumor therapies because of its role in angiogenesis[5-6]. Aptamers are short, single-stranded DNA or RNA oligonucleotides, and produced by phylogenetic evolution of the ligand using the exponential enrichment (SELEX) method. Aptamers are similar to antibodies whose have high affinity and specificity towards their targets[7]. Due to their unique properties, aptamers play an important role in the targeted delivery of chemotherapeutic agent, siRNA, and drug-loaded nanoparticles. Gint4.T is an RNA-aptamer that can specifically bind to PDGFRβ and is also a PDGFRβ-specific antagonist [8].

DNA is an ideal material for nanostructure construction because the assembly can be precisely controlled by Waston-Crick base paring[9]. To date, a number of

two-dimensional (2D) and three-dimensional (3D) DNA nanostructures have been designed and demonstrated[10-12]. Tetrahedral DNA nanostructures (TDN) have attracted significant attention because of their biocompatibility, stability, abundant functionalized modification sites, and low immunogenicity[13-15]. Turberfield et al. synthesized DNA tetrahedral nanostructures with high yield using a one-step synthesis method. [16]. Walsh et al. found that nucleic acid probe DNA tetrahedra can enter mammalian cells without the need for a transfection reagent[17]. Lee et al. demonstrated that self-assembled tetrahedral nanoparticles can be used for targeted siRNA delivery in vivo[18]. TDN have shown excellent application prospects for molecular diagnostics, molecular delivery, and targeted drug therapy. In this study, we report a novel drug-loaded system that combines the Gint4.T aptamer and TDN. The Gint4.T modified DNA tetrahedron can enhance specific cellular uptake and cytotoxicity against U87MG cells.

Methods

Material

All DNA oligonucleotides and 2'F-Py RNA oligonucleotides were purchased from Sangon Biotech (Shanghai, China) and all oligonucleotide sequences are listed in Table 1. GelRed DNA gel stain solution was purchased from Sangon Biotech (Shanghai, China). Fetal bovine serum(FBS) and Dulbecco's modified Eagle's medium (DMEM) were both purchased from Thermo Fisher(New York, USA). Doxorubicin (Dox) was purchased from Mengbio Technology(Chongqing, China). U87 cell lines were purchased from Shanghai Life Academy of Sciences Cell Library (Shanghai, China). DAPI were purchased from Zhongshan Golden Bridge Biotechnology (Beijing, China).

Preparation of DNA nanostructures

To assemble the DNA tetrahedron (Table 1), 2 uL of each oligonucleotide (S1, S2, S3 and S4) was added to 42 μL of a TM buffer (10 mM Tris-HCl, 5mM $MgCL_2$, pH

=8).The DNA solution was then heated to 95°C for 5 min and subsequently cooled to 4°C for 2 min using a Bio-rad PCR machine (California, USA)[19, 20]. The final concentration of TDN was 2 uM. TDN' was prepared by the same manner except S1 was replaced by S1'. To synthesize the Gint4.T aptamer modified TDN (Apt-TDN), the Gint4. T aptamer was added in an equal molar ratio with TDN' and incubated at 37°C for 60 min. Before synthesis, the aptamer was subjected to a short denaturation-renaturation step (85°C for 5 min, rapidly cooled in 2 min and subsequently warmed to 37°C for 10min)[21].

Agarose gel electrophoresis

An agarose gel (3%) was run in 0.5X TEB buffer at 100V for 30 min. The temperature of the electrophoresis was maintained at 0°C by placing the apparatus in an ice bath. Before electrophoresis, Gel Red was added to the agarose gel to stain the DNA strands. When the process was finished, Bio-rad fluorescence scanner(California, USA)was used to capture the gel image.

Dynamic light scattering (DLS)

Malvern Zetasizer ZS90 (Malvern, UK) was used to measure the hydrodynamic sizes and zeta-potentials of the TDN. A total of 1 mL of the TDN (100 nM) was subjected to the DLS analysis.

Atomic force microscopy (AFM) imaging

The TDNs were diluted to 100 nM with TM(including $MgCl_2$ and Tris-Hcl buffer). Then 10 μL of the TDN samples was added onto freshly cleaved mica for 10 min. The samples were subsequently imaged in AC mode on an AFM instrument(Agilent 5500, USA).

Measurement of the drug loading capacity of the prepared TDN

Doxorubicin was dissolved in deionized water to make a 500μM concentration storage solution. Different concentration of doxorubicin (1 to 20 μM) was mixed with

TDN (100 nM) and Apt-TDN (100 nM) for 6 h at room temperature (24°C-26°C). The mixed solution was then centrifuged at 12000g for 10 min to obtain the drug-loaded TDN. Then 50 μL of the supernatants were removed and mixed with PBS by 1:1 ratio. Varioskan lux microplate reader (California, USA) was used to measure the fluorescence intensity of doxorubicin (λ_{ex} = 480 nm and λ_{em} = 590 nm) to determine the amount of doxorubicin in the supernatants.[22].The concentration of doxorubicin loaded in the TDN was calculated by the standard curve and fluorescence intensity

.

Serum stability of the TDN in vitro

The TDN was mixed with complete media at 37°C for 0, 2, 4, 6, 8, 10, 12, and 24 h. The TDN solutions were mixed with FBS at a 1:1 ratio and incubated at 37°C for 1, 3, 5, or 7 h. After incubation, the mixture was run in 3% agarose gel.

Cytotoxicity of the TDN in vitro

To determine the cytotoxicity, U87MG cells at a concentration of $1*10^4$ were seeded onto a 96-well plate. The cell culture medium was removed and fresh media containing 0-500 nM TDN was added for another 24 h and 48 h of incubation after overnight incubation. Then, 10 μL of CCk-8 solution was added to each well and the mixture was incubated for 1 h. The absorbance was then measured at 450 nm using a microplate reader.

Fluorescence imaging

Celluar uptake of DOX and TDN were studied by fluorescence microscopy(Olympus, Tokyo, Japan). U87MG cells were seeded on cover slips in 24-well plates with medium containing 10% heat-inactivated fetal bovine serum and 1% penicillin and streptomycin for at least 1 day at 37 °C in a humidified atmosphere with 5% CO_2 until cells reached at least 75% of the space. After incubation, culture media was removed. Complete media containing 100 nM of Cy3-TDN and Cy3-Atp-TDN was added and incubated for 3 h. TDN and Apt-TDN were labeled with Cy3 to detect the

intercellular uptake of nanoparticals. For the celluar uptake of DOX, DOX(DOX:2μM), DOX@TDN (DOX:2μM) and DOX@Apt-TDN(DOX:2μM) were added to U87MG cells and incubated with 3 h. After 3 h treatment, cells were fixed with 4% paraformaldehyde for 20 min in dark place and subsequently stained with 4', 6-diamidino-2-phenylindole (DAPI) for 5 min. Cells was washed with PBS three times and observed under a fluorescence microscope.

Flow cytometry

$1*10^6$ U87MG cells were implanted into 6-well plates. After overnight incubation, culture media was removed and media treated with 100 nM Cy3-TDN, 100 nM Cy3-Atp-TDN and 100 nM Cy3-Atp-TDN+ 1μM free Atp was added and incubated for 3 h. Then, the cells were fixed with 4% paraformaldehyde for 20 min, and flow cytometry was used to analyze the percentages of Cy-3 positive cells.

Cell cycle and apoptosis

After treated with Dox, Dox-TDN and Dox-Atp-Dox-TDN for 24h, $5*10^5$ cells were collected and fixed in 75% icecold ethanol overnight. Then cells were incubated with RNase and propidium iodide for 30 min at 37℃ in the dark. The cell cycle was investigated by flow cytometry. In addition, after various treatments, the cells were stained with AnnexinV-FITC/DAPI, and the early apoptosis were explored.

CCK-8 Assays

U87MG cells ($5x10^3$) were seeded onto 96-well plates to determine cell viability, with 100 μL of media and cultured overnight at 37 °C under an atmosphere containing 5% CO_2. The medium was subsequently removed and fresh medium containing Dox, Dox-TDN, or Dox-Apt-TDN was added. After 24 h of incubation, 10μL of a CCK-8 solution was added and the cells were cultured for another 1 h. Microplate reader was used to measure the absorbance at 450 nm.

Statistical Analysis

All experiments were performed in triplicate in this study and all data are presented as a mean value with its standard deviation indicated (mean ± SD).Statistical analysis was performed using the SPSS 24.0 program (IBM, USA). Significant differences were determined using the Student's *t* test with a $P<0.05$ indicating significant differences between groups.

Results

Synthesis and characterization of TDN and Apt-TDN

The TDN was self-assembled from four oligonucleotides (Table 1) via single-step synthesis as previously reported[23, 24]. The tumor targeting aptamer Gint4.T was used to modify TDN via Watson-Crick base pairing. The DNA tetrahedron contains four faces with each face formed by one oligonucleotide. Thus, four oligonucleotides combined with each other to form a DNA tetrahedron by hybridization (Figure 1a). Gel electrophoresis analysis showed a single prominent band on Lanes 4 and 5, suggesting that the TDN and Apt-TDN were successfully constructed. The mobility of the Apt-TDN decreased compared to that of the TDN, suggesting that the Gint4.T aptamer successfully modified the TDN.

The sizes of the TDN and Apt-TDN were determined by DLS and AFM. The TDN and Apt-TDN showed particle sizes of 10.1 nm and 13.5 nm, respectively, reflecting the addition of the Gint4.T ligand (Figure 1b-A.B). Because the hydrodynamic diameter included water molecules, the particles were larger than theory. The heights of the TDN and Apt-TDN determined by AFM images were both ~2 nm(Figure 1-c), indicating that aptamer modification did not change the 3D structure formation. The average zeta potentials of the TDN and Apt-TDN were -5.69mV (C) and -7.3mV (D), respectively (Figure 1b-C.D). Based on these parameters, we concluded that the TDN and Apt-TDN were successfully assembled.

Stability and cytotoxicity of TDN in vitro

Gel electrophoresis results showed that the TDN remained intact in complete media

for 24 h when incubated at 37°C (Figure 2a-A). Furthermore, when the concentration of fetal bovine serum was increased to 50%, the TDN remained stable for at least 7 h (Figure 2a-B), which is consistent with previous reports[19, 24]. To determine the cytotoxicity of the nanostructure, CCK-8 assays were used to assess the cell viability of U87 cells after treatment with a number of TDN concentrations. From Figure 2b, no significant cytotoxicity was observed for the TDNs in U87 cells at 0–500nM after 24 h and 48h. Hence, DNA nanoparticals can be used as a stable and bio-safe cargo for drug delivering.

Drug loading capacity of the TDN and Apt-TDN

Doxorubicin is a broad-spectrum chemotherapeutic drug that can intercalate into DNA double strands. We calculated a standard curve of Doxorubicin(Figure 3a) and then investigated the intercalation of doxorubicin into TDN. The amout of interclated doxorubicin in TDN and Apt-TDN gradually increases with increasd concentration of doxorubicin. When the doxorubicin concentration was 14 μM, the intercalation peaked at 5.5 μM and 6.0 μM respectively and subsequently plateaued (Figure 3b), indicating that the DNA strands were fully occupied. Meantimes, we also scanning the fluorescence spectrum of doxorubicin in the supernant. The fluorescence of doxorubicin was quenched at 14 μM(Figure 3c). Based on those facts, we concluded that approximately 55 molecules of doxorubicin were associated within a single TDN, while 60 molecules within a single Apt-TDN.

Targeted cellular uptake of Apt-TDN

DNA is a negatively charged macromolecule that makes it difflicult to enter the same negatively charged cell membance. Typically, individual DNA molecules need to be able to access cells with the help of transfection reagents. Here, we labeled TDN and Apt-TDN with Cy3 for the incellular uptake of the nanoparticals. After incubated with U87MG cells for 3 h, the red cy3 fluorescence signal emerged in the cellular cytoplasm, which meas TDNs can bind to cytomembrane and be uptaken into the cell without the help of transfection agents (Fig 4a). Apt-TDN showed higher red

fluoreccence, which suggests that the presence of the Gint4.T aptamer significantly increased the DNA tetrahedron uptake by U87MG cells. However, when added free aptamer, the cy3 fluorescence was decreased to the level of TDN. We infer that due to the competitive inhibition by the free aptamer, aptamer on the TDN can not facilitate the uptake of TDN. Based on the competive inhibition, we proved that the Apt-TDN can targed the U87MG cells. Flow cytometry further proved that the cy3 positive percentages of U87MG cells were higher in Apt-TDN group than that of TDN group. Free Apt could decrease the cy3 positive percentages in Apt-TDN group(Figure 4b).

Cellular uptake of the DOX@TDN and DOX@Apt-TDN

We utilizing the charscteristic fluorescence spectrum of doxrubicin for the drug uptake efficiency. After 3 h treatment, the intracellular of doxorubicin was imaged by fluoresece(Figure 5a). Free doxorubicin can enter the U87MG cell and located in the nucleus.When added DOX@TDN, the fluorescence was higher than that of free doxorubicin. That suggested that the DNA nanoparticals can enhance the cellular uptake of doxorubicin. When added DOX@Apt-TDN, the red signal in the nucleus was even higher than that of DOX@TDN. Semi-quantity analysis of intracellular uptake of DOX furether confirm that Apt-TDN can more than two folds of drug than single drug alone. We infer that due to the Gin4.T specific binding to receptors, more nanoparticals can enter into the cell. After digested in the lysosomes, doxorubicin can be released into the cytoplasm and futher acts into the nucleus.

Cytotoxicity of Dox, Dox@TDN and Dox@Apt-TDN

For the cytotoxicity study, three groups of different concentrations of doxorubicin were used on U87MG cell(Figure 6a). The IC_{50} values were 13.39 μM for DOX, 7.826 μM for DOX@TDN and 4.205 μM for DOX@Apt-TDN. Among the three groups, Apt-TDN showed the highest cytotoxicity at 24h, which indicated that Apt-TDN had its specificity to U87MG cells. After 24h, the cells in DOX, Dox@TDN and Dox@Apt-TDN group were collected to explore early apoptosis. Our data demonstrated that the early apoptosis rates were highest in Dox@Apt-TDN

group than that in other two groups(Figure 6b).

Discussion

Whether in vitro or in vivo experiments, the stability of drug and carrier must be determined. After assembling the TDNs, their stability was first determined in vitro. This study showed that the 3D structure of the DNA nanoparticles can improve their stability in serum by inhibiting enzyme binding. The biological safety of the relevant nanostructures is the most important requirement for their application. No significant cytotoxicity was observed in various concentrations of TDN co-cultured with U87 cells for 24 hours and 48h. None of the DNA sequences used in this study encode any genetic information and no side effects were reported in the cytotoxicity test. Therefore, the TDNs can serve as a safe and stability drug carrier.

The targeting efficiency of the aptamer-modified nanostructure is crucial for selective drug delivery to cancer cells. Compared to antibodies, aptamers are chemically stable, inexpensive, and can be mass-produced. Compared with other materials, aptamers can easily bind to DNA tetrahedra using the principle of base complementary pairing. Thus, the foundation for targeted drug delivery and next-generation treatments have been laid by the combination between aptamers and DNA tetrahedron. Our study demonstrates that the Gint4.T aptamer can target U87MG cells due to the high expression of PDGGRβ on the surface of glioma cells. Camorani et al.[8] also showed that the Gint4.T aptamer could target tumor cells by specifically interactings with the extracellular domain of the PDGFRβ. Advantages of Gint4.T aptamer targeting have been demonstrated to some extent via in vitro studies, but requires further in -vivo testing to confirm. This study also confirmed that the DOX@Apt-TDN were more cytotoxic than DOX and DOX@TDN, which likely priginates from two factors.First, Gint4.T aptamers can specifically bind to PDGFR extracellular domains, blocking tumor cell proliferation and inhibiting tumor cell growth[8]. In addition, Gint4.T specifically binds to tumor cells and enhances the cell targeting of the DOX@Apt-TDN complex. Thus, we can increase the targeting of drugs and reduce the dose of systemic administration dose to prevent systemic side effects of anti-tumor

drugs.

Conclusion

In conclusion, we assembled functional TDN by conjugation with the Gint4.T aptamer. The stability of the DNA nanostructure in serum enables its use as a drug delivery vehicle. Modification with Gint4.T increases the specificity and efficiency of antitumor drugs by targeting the PDGFRβ receptor in vitro. Compared with Dox@TDN, Dox@Apt-TDN significantly enhanced the cytotoxicity towards U87MG cells. The Gint4.T modified DNA tetrahedron enhanced specific cellular uptake and cytotoxicity against U87MG cells. Gint4.T target PDGFRβ can synergize with doxorubicin to enhance anti-glioma effect. This study demonstrated that the aptamer modified nanostructure can provide a novel therapy tool for the treatment of brain tumors. Gint4.T should be an excellent aptamer for glioma targeted therapy due to the high expression of PDGFR in glioma cells. And DNA tetrahedron can be a high-efficiency targeted drug delivery system suitable for brain tumor treatment due to its biocompatibility, loading efficiency, and safety.

Availability of Data and Materials

The relevant data are included within the article.

Conflicts of interest

The authors declare no conflict of interest.

Funding

This work was supported by grants from the National Natural Science Foundation of China (No: 81201066, 81371674).

Acknowledgements

The authors thank Prof Weiwei Zhang and Prof Haizhong Feng (Shanghai Jiao Tong University) for kindly providing U87-EGFRvIII.

Authors' information

[1]Department of Neurosurgery, the Second Affiliated Hospital of Chongqing Medical University, Chongqing, 400010, China.

[2]Department of Orthopedics, the Second Affiliated Hospital of Chongqing Medical University, Chongqing, 400010, China.

[3]Department of Neurology, Chongqing General Hospital, Chongqing, 400013, China.

References

1. Tan Y, Li QM, Huang N, et al (2017) Upregulation of DACT2 suppresses proliferation and enhances apoptosis of glioma cell via inactivation of YAP signaling pathway. Cell Death Dis 8:e2981. https://doi.org/10.1038/cddis.2017.385
2. Siegel RL, Miller KD, Jemal A, et al (2016) Cancer Statistics, 2016. CA Cancer J Clin 66:7–30. https://doi.org/10.3322/caac.21332.
3. Mangiola A, Anile C, Pompucci A, et al (2010) Glioblastoma therapy : going beyond Hercules Columns. 2010. Expert Rev Neurother. 10:507-14. http://doi.org/10.1586/ern.09.158
4. Polley MYC, Lamborn KR, Chang SM, et al (2011) Conditional probability of survival in patients with newly diagnosed glioblastoma. J Clin Oncol 29:4175–4180. https://doi.org/10.1200/JCO.2010.32.4343
5. Kim Y, Kim E, Wu Q, et al (2012) Platelet-derived growth factor receptors differentially inform intertumoral and intratumoral heterogeneity. Genes Dev 26:1247–1262. https://doi.org/10.1101/gad.193565.112
6. Appiah-Kubi K, Wang Y, Qian H, et al (2016) Platelet-derived growth factor receptor/platelet-derived growth factor (PDGFR/PDGF) system is a prognostic and treatment response biomarker with multifarious therapeutic targets in cancers. Tumor Biol 37:10053–10066. https://doi.org/10.1007/s13277-016-5069-z
7. Tang J, Huang N, Zhang X, et al (2017) Aptamer-conjugated PEGylated quantum dots targeting epidermal growth factor receptor variant III for fluorescence imaging of glioma. Int J Nanomedicine 12:3899–3911. https://doi.org/10.2147/IJN.S133166

8. Camorani S, Esposito CL, Rienzo A, et al (2014) Inhibition of receptor signaling and of glioblastoma-derived tumor growth by a novel PDGFRβ aptamer. Mol Ther 22:828–841. https://doi.org/10.1038/mt.2013.300

9. Goodman RP, Schaap IAT, Tardin CF, et al (2005) Rapid chiral assembly of rigid DNA building blocks for molecular nanofabrication. Science 310:1661–1665. https://doi.org/10.1126/science.1120367

10. Douglas SM, Dietz H, Liedl T, et al (2009) Self-assembly of DNA into nanoscale three-dimensional shapes. Nature 459:414–418. https://doi.org/10.1038/nature08016

11. Andersen ES, Dong M, Nielsen MM, et al (2009) Self-assembly of a nanoscale DNA box with a controllable lid. Nature 459:73–76. https://doi.org/10.1038/nature07971

12. Barrow SJ, Funston AM, Wei X, Mulvaney P (2013) DNA-directed self-assembly and optical properties of discrete 1D, 2D and 3D plasmonic structures. Nano Today 8:138–167. https://doi.org/10.1016/j.nantod.2013.02.005

13. Keum J-W, Bermudez H (2009) Enhanced resistance of DNA nanostructures to enzymatic digestion. Chem Commun 7036. https://doi.org/10.1039/b917661f

14. Li J, Pei H, Zhu B, et al (2011) Self-assembled multivalent DNA nanostructures for noninvasive intracellular delivery of immunostimulatory CpG oligonucleotides. ACS Nano 5:8783–8789. https://doi.org/10.1021/nn202774x

15. Pinheiro A V, Han D, Shih WM, Yan H (2011) Challenges and opportunities for structural DNA nanotechnology. Nat Publ Gr 6:763–772. https://doi.org/10.1038/nnano.2011.187

16. Goodman RP, Berry RM, Turberfield AJ (2004) The single-step synthesis of a DNA tetrahedron. Chem Commun (Camb) 44:1372–1373. https://doi.org/10.1039/b402293a

17. Walsh AS, Yin H, Erben CM, et al (2011) DNA cage delivery to mammalian cells. ACS Nano 5:5427–5432. https://doi.org/10.1021/nn2005574

18. Lee H, Lytton-Jean AKR, Chen Y, et al (2012) Molecularly self-assembled nucleic acid nanoparticles for targeted in vivo siRNA delivery_Lee et al._2012.pdf. Nat Nanotechnol 7:389–393. https://doi.org/10.1038/nnano.2012.73

19. Jiang D, Sun Y, Li J, et al (2016) Multiple-Armed Tetrahedral DNA Nanostructures for Tumor-Targeting, Dual-Modality in Vivo Imaging. ACS Appl Mater Interfaces 8:4378–4384. https://doi.org/10.1021/acsami.5b10792

20. Xia Z, Wang P, Liu X, et al (2016) Tumor-Penetrating Peptide-Modified DNA Tetrahedron for Targeting Drug Delivery. Biochemistry 55:1326–1331. https://doi.org/10.1021/acs.biochem.5b01181

21. Monaco I, Camorani S, Colecchia D, et al (2017) Aptamer Functionalization of Nanosystems for Glioblastoma Targeting through the Blood-Brain Barrier. J Med Chem 60:4510–4516. https://doi.org/10.1021/acs.jmedchem.7b00527

22. Kim KR, Kim HY, Lee YD, et al (2016) Self-assembled mirror DNA nanostructures for tumor-specific delivery of anticancer drugs. J Control Release 243:121–131. https://doi.org/10.1016/j.jconrel.2016.10.015

23. Erben CM, Goodman RP, Turberfield AJ (2006) Single-molecule protein encapsulation in a rigid DNA cage. Angew Chem Int Ed Engl 45:7414–7417. https://doi.org/10.1002/anie.200603392

24. Tian T, Li J, Xie C, et al (2018) Targeted Imaging of Brain Tumors with a Framework Nucleic Acid Probe. ACS Appl Mater Interfaces 10:3414-3420. https://doi.org/10.1021/acsami.7b17927

Table 1: Sequence of each single strand DNA and RNA

ssDNA	DNA and RNA Sequence(5'→3')
S1	ACATTCCTAAGTCTGAAACATTACAGCTTGCTACACGAGAAGAGCCGC CATAGTA
S1'	TTTTTTACATTCCTAAGTCTGAAACATTACAGCTTGCTACACGAGAAGA GCCGCCATAGTA
S2	TATCACCAGGCAGTTGACAGTGTAGCAAGCTGTAATAGATGCGAGGG TCCAATAC
S3	TCAACTGCCTGGTGATAAAACGACACTACGTGGGAATCTACTATGGCG GCTCTTC
S4	TTCAGACTTAGGAATGTGCTTCCCACGTAGTGTCGTTTGTATTGGACC CTCGCAT
cy3-S2	cy3-TATCACCAGGCAGTTGACAGTGTAGCAAGCTGTAATAGATGCGAG GGTCCAATAC
Gint4.T	UGUCGUGGGGCAUCGAGUAAAUGCAAUUCGACAAAAAAA

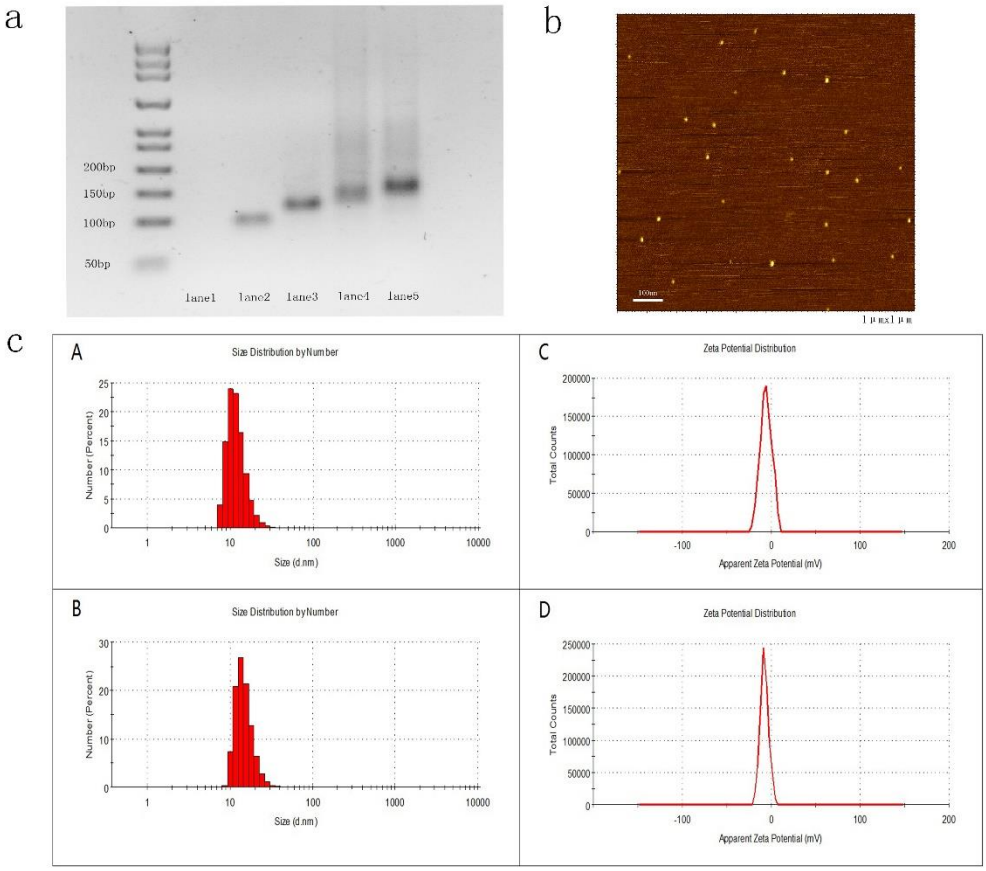

Figure 1: (a)Synthesis of the DNA tetrahedron and Gint4. T-TDNs. Lane 1: S1; lane 2: S1+S2; lane 3: S1+S2+S3; lane 4: S1+S2+S3+S4 (TDN); lane 5: TDNs mixed with Apt-tail (Gint4.T); Apt-TDN. Lane 1 was not visible because nucleic acid dyes cannot properly stain single strand DNA. (b)AFM images showed that the heights of the TDN and Apt-TDN were ~2nm.(c)Determination of the particle size and zeta potential of TDN and Apt-TDN by dynamic light scattering (DLS). The average particle sizes of the TDN and Apt-TDN were 10.10 nm (A) and 13.54 nm (B), respectively. The average zeta potentials of the TDN and Apt-TDN were -5.69 mV (C) and -7.3 mV (D), respectively.

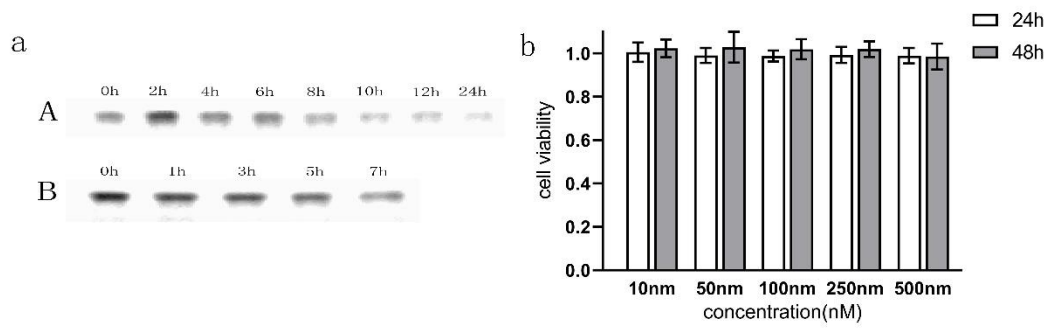

Figure 2: (a)Gel electrophoresis results showed that the TDN remained stable for 24 h in complete media at 37°C (A); increasing concentration of fetal bovine serum to 50% and the TDN remained stable for 7 h (B).(b) U87MG cells were co-cultured with different concentrations (10–500 nM) of TDN for 24 h and 48h. The CCK-8 assay showed that the activity of the U87 cells was not affected, which indicated reliable biosafety of the TDN.

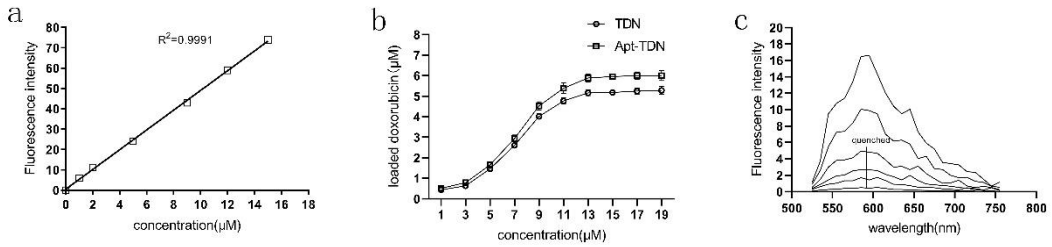

Figure 3:(a)A standard curve of Dox concentrations in PBS buffer, λex = 480 nm and λem = 590 nm The amount of Dox carried by TDN and Apt-TDN.(b)Dox was inserted into the DNA double strand of the TDN and Apt-TDN. When the Dox concentration reached 14 μM and the inserted Dox reached a peak of 5.5 μM and 6.0μM, thus a single DNA tetrahedron could carry 55 Dox molecules, while a single Aptamer modified DNA tetrahedron carries 60 Dox molecules. (c)Fluorescence spectra of Dox in the supernatant. When added 14 μM doxorubicin, the fluorescence was quenched.

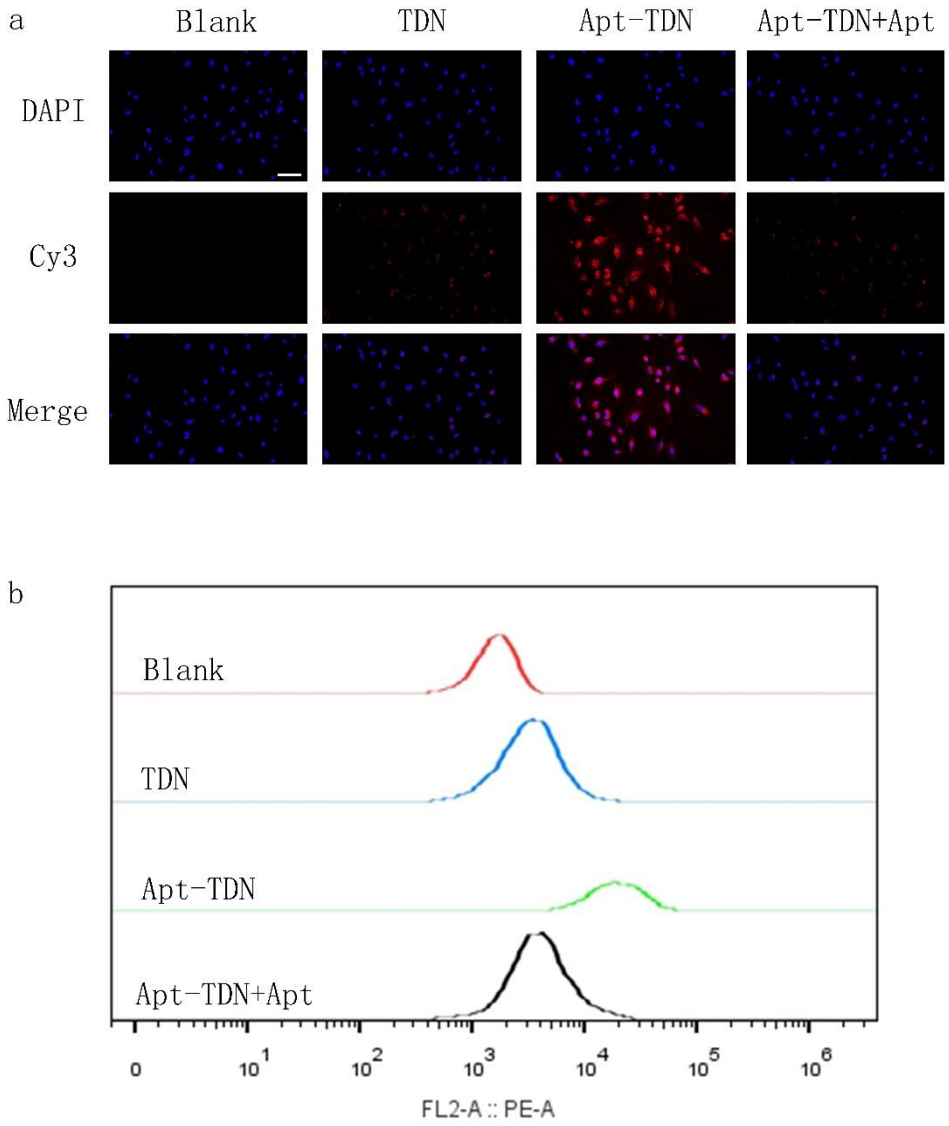

Figure 4:(a)U87 cells uptake of the TDN and Apt-TDNs (TDN-Gint4.T). TDNs enter U87 cells directly without transfection agents and the uptake of Apt-TDN (linked to aptamer Gint4.T) significantly increased, the uptake of Apt-TDNs by U87 cells were competitively inhibited by free Apt(Gint4.T), those data indicate that the aptamer Gint4.T plays a significant role in cellular targeting. The scale bar are 50 μm.(b) Flow cytometry curves shows the intracellular uptake of TDN, Apt-TDN and Apt-TDN+Apt after incubation for 3 h.

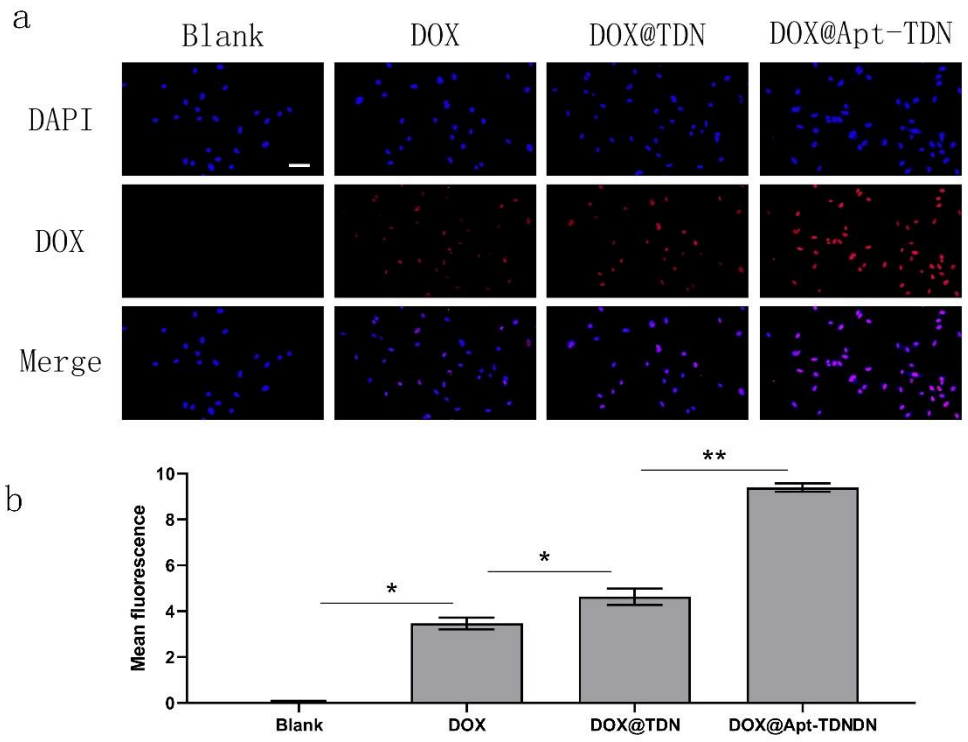

Figure 5:(a)Cellular uptake of DOX, DOX@TDN, DOX@Apt-TDN. Modified by the Gint4.T aptamer, Apt-TDN can deliver more doxorubicin to U87MG cells than TDN. Besides, the TDN can also carry more drug to cell than single drug alone. The scale bar values are 50 μm.(b)Semi-quantitative analysis of fluorescence intensity of doxorubicin when treated with PBS, DOX, DOX@TDN and DOX@Apt-TDN. Statistical analysis:*P<0.05,**<0.01.

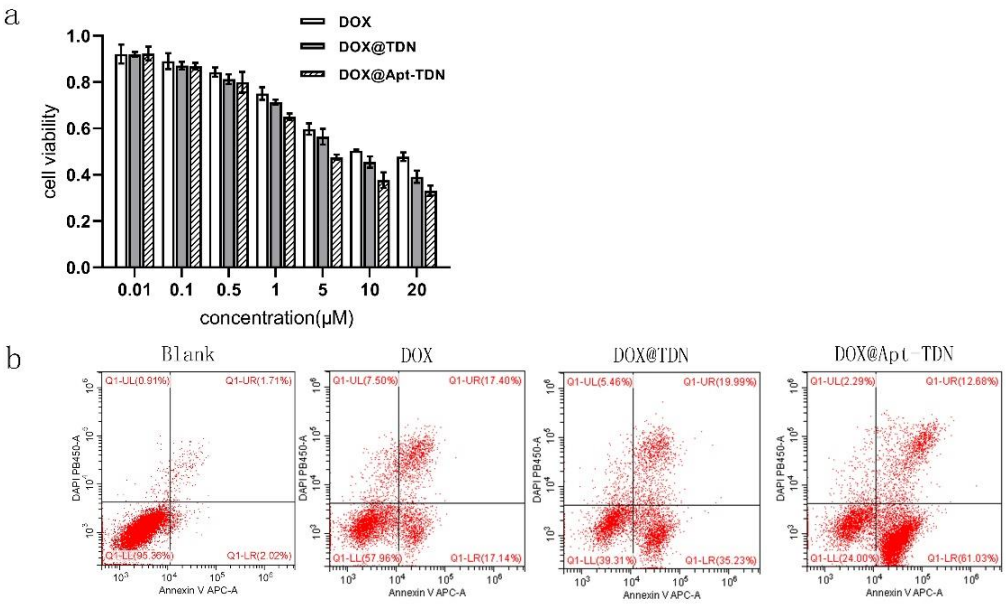

Figure 6:(a)Cytotoxicity of DOX, DOX@TDN, and DOX@Apt-TDN at various concentrations. The inhibition rate of the U87 cells increased significantly with increasing of DOX concentration, but at the same concentration, the DOX@TDN and DOX@Apt-TDN groups significantly increased cytotoxicity compared with the DOX group alone. The cell inhibition rate of the DOX@Apt-TDN group was also significantly higher than that of the DOX@TDN group ($p<0.05$).(b)Apoptotic statistics of U87MG cell after incubation with PBS, DOX, DOX@TDN, DOX@Apt-TDN for 24 h. (c)Flow cytometry histograms of U87MG cell cycle after incubation with PBS, DOX@TDN, DOX@Apt-TDN for 24 h.

Figures

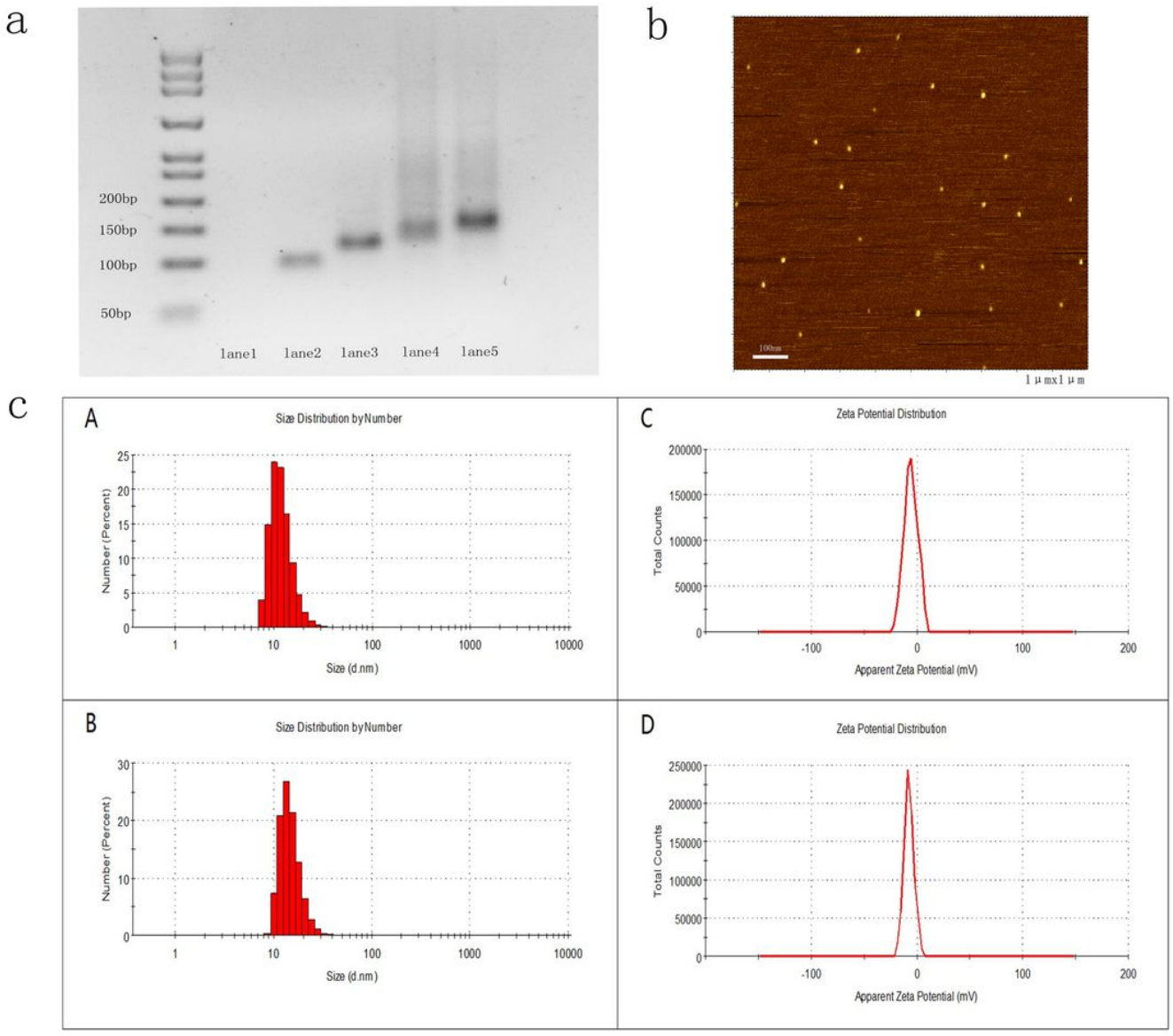

Figure 1

(a Synthesis of the DNA tetrahedron and Gint4. T TDNs. Lane 1: S1; lane 2: S1+S2; lane 3: S1+S2+S3; lane 4: S1+S2+S3+S4 (TDN); lane 5: TDNs mixed with Apt tail (Gint4.T); Apt TDN. Lane 1 was not visible because nucleic acid dyes cannot properly stain single strand DNA. (b AFM images showed that the height s of the TDN and Apt TDN were ~ c Determination of the particle size and zeta potential of TDN and Apt TDN by dynamic light scattering (DLS). The average particle sizes of the TDN and Apt TDN were 10.10 nm (A) and 13.54 nm (B), respectively. The average zeta potentials of the TDN and Apt TDN were 5.69 mV (C) and 7.3 mV (D)),

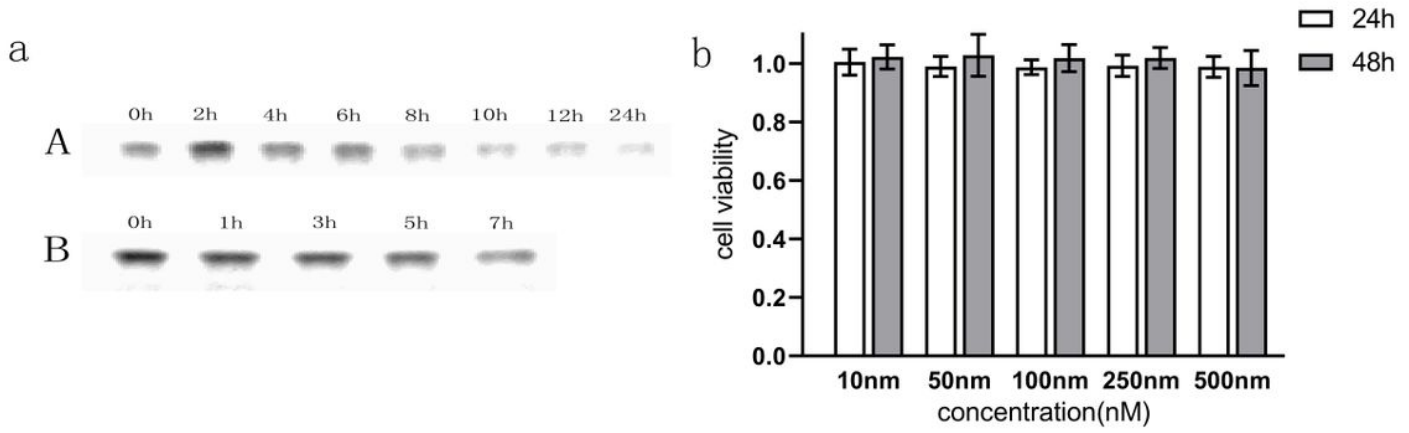

Figure 2

a Gel electrophoresis results showed that the TDN remain ed stable for 24 h in complete medi a at 37 °C (A); increas ing concentration of f e tal bovine serum to 50% and the TDN remain ed stable for 7 h (b U87MG cells were co cultured with different concentrations (10 500 nM) of TDN for 24 h and 48h . The CCK 8 assay showed that the activity of the U87 cells was not affected, which indicated reliable biosafety of the TDN.

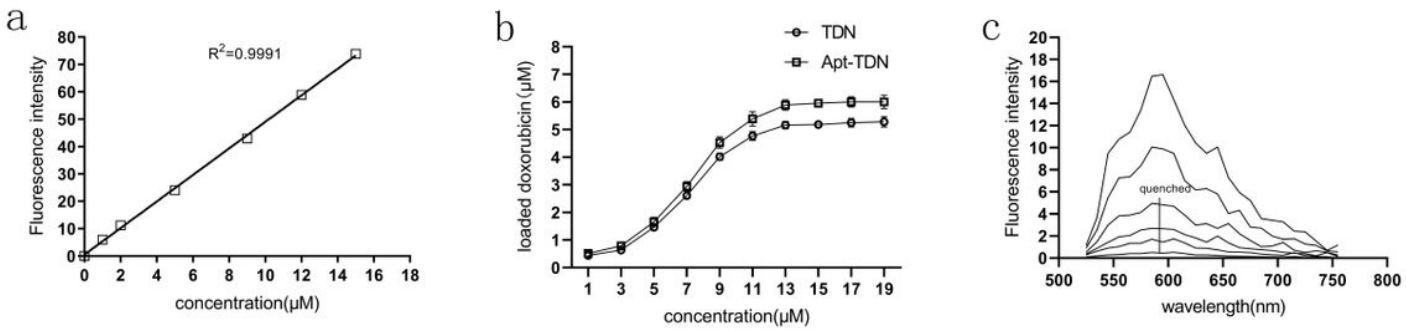

Figure 3

A standard curve of Dox concentrations in PBS buffer , λex = 480 nm and λem = 590 nm The amount of Dox carried by TDN and Apt TDN.(b)Dox was inserted into the DNA double strand of the TDN and Apt TDN . Wh en the Dox concentration reache d 14 μ M and the inserted Dox reache d a peak of 5.5 μ M and 6.0 μ M, thus a single DNA tetrahedron c ould carry 55 Dox molecules , while a single Aptamer modified DNA tetrahedron carries 60 Dox molecules (Fluorescence spectra of Dox in the supernatant . When added 14 μ M doxorubicin, the fluorescence was quenched

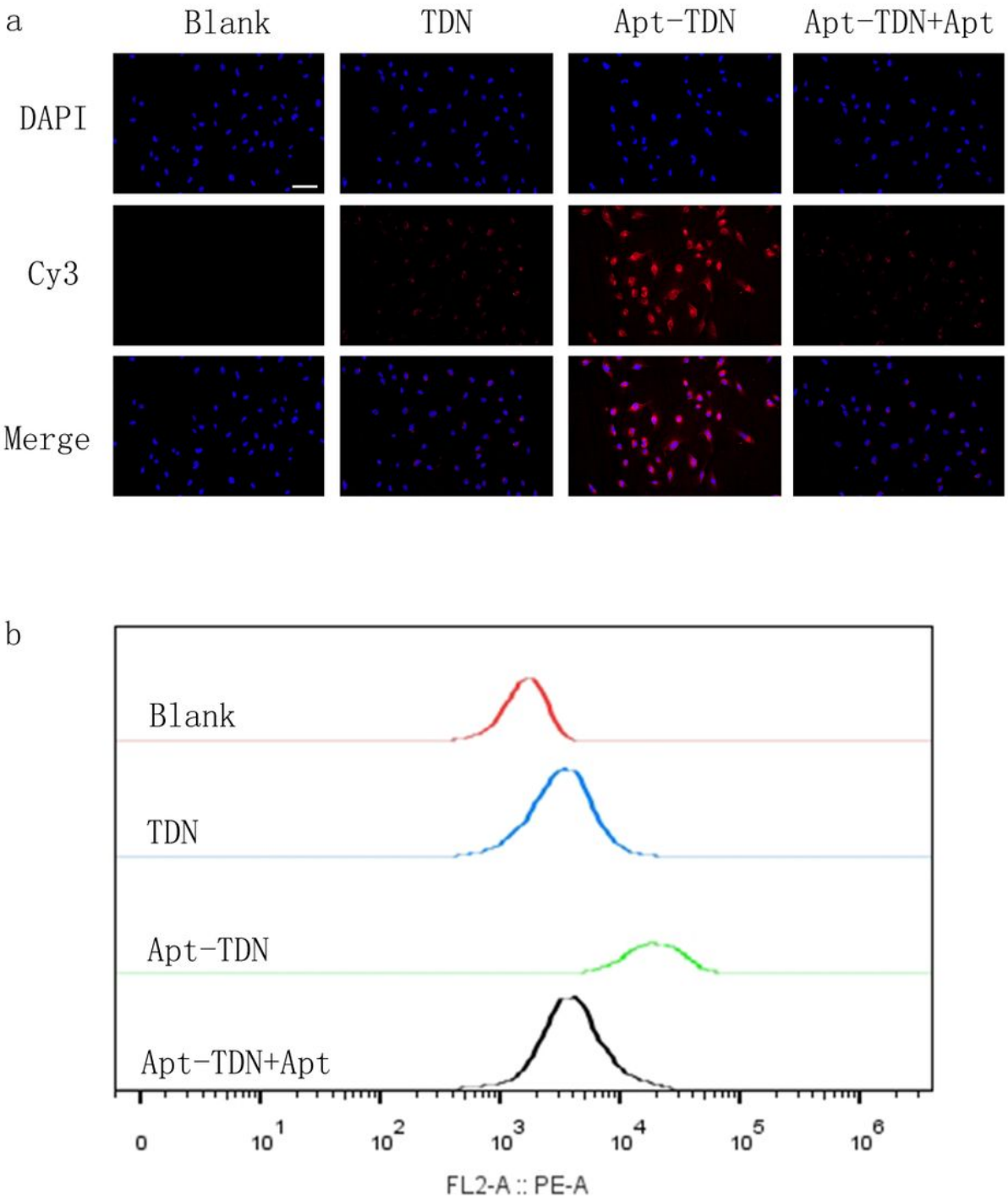

Figure 4

(U87 cells uptake of the TDN and Apt TDNs (TD N Gint4.T). TDNs enter U87 cells directly without transfection agents and the uptake of Apt TDN (linked to aptamer Gint4.T) significantly increased, the uptake of Apt TDN s by U87 cells were competitively inhibit ed by free Apt(Gint4.T), those data indicat e that the aptamer Gint4.T plays a significant role in cellular targeting. The scale bar are 50 μm. b) Flow

cytometr y curves shows the intracellular uptake of TDN, Apt TDN and Apt TDN+Apt after incubation for 3 h

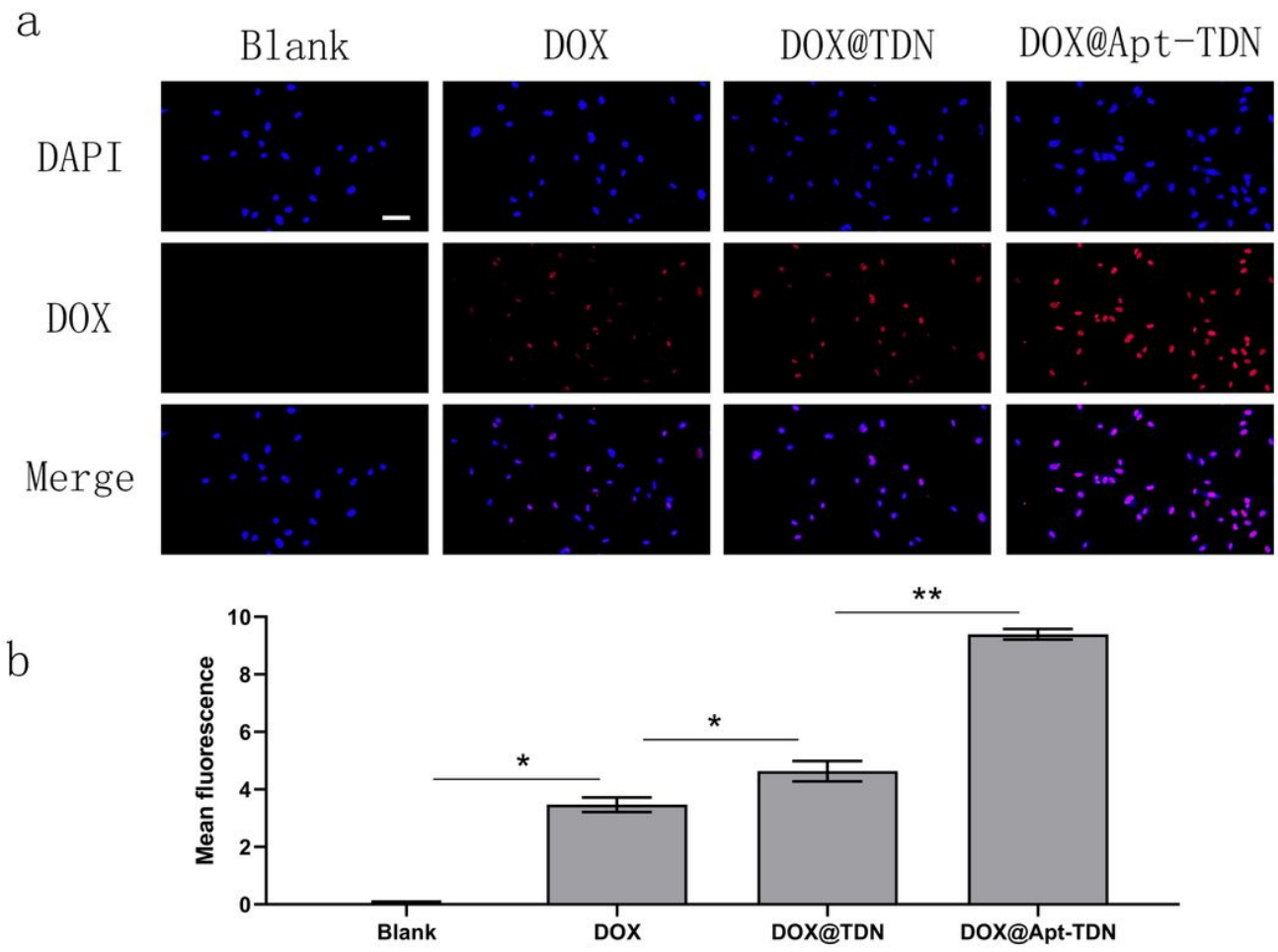

Figure 5

a) Cellular uptake of DOX, DOX@TDN, DOX@Apt TDN. Modified by the Gint4.T aptamer, Apt TDN can deliver more doxorubicin to U87MG cells than TDN. Be sides, the TDN can also carry more drug to cell than single drug alone. The scale bar values are 50 μm. b)Semi quantitative analysis of fluorescence intensity of doxorubicin when treated with PBS, DOX, DOX@TDN and DOX@Apt TDN. Statistical analysis :*P<0.05 ,**<0.01.>

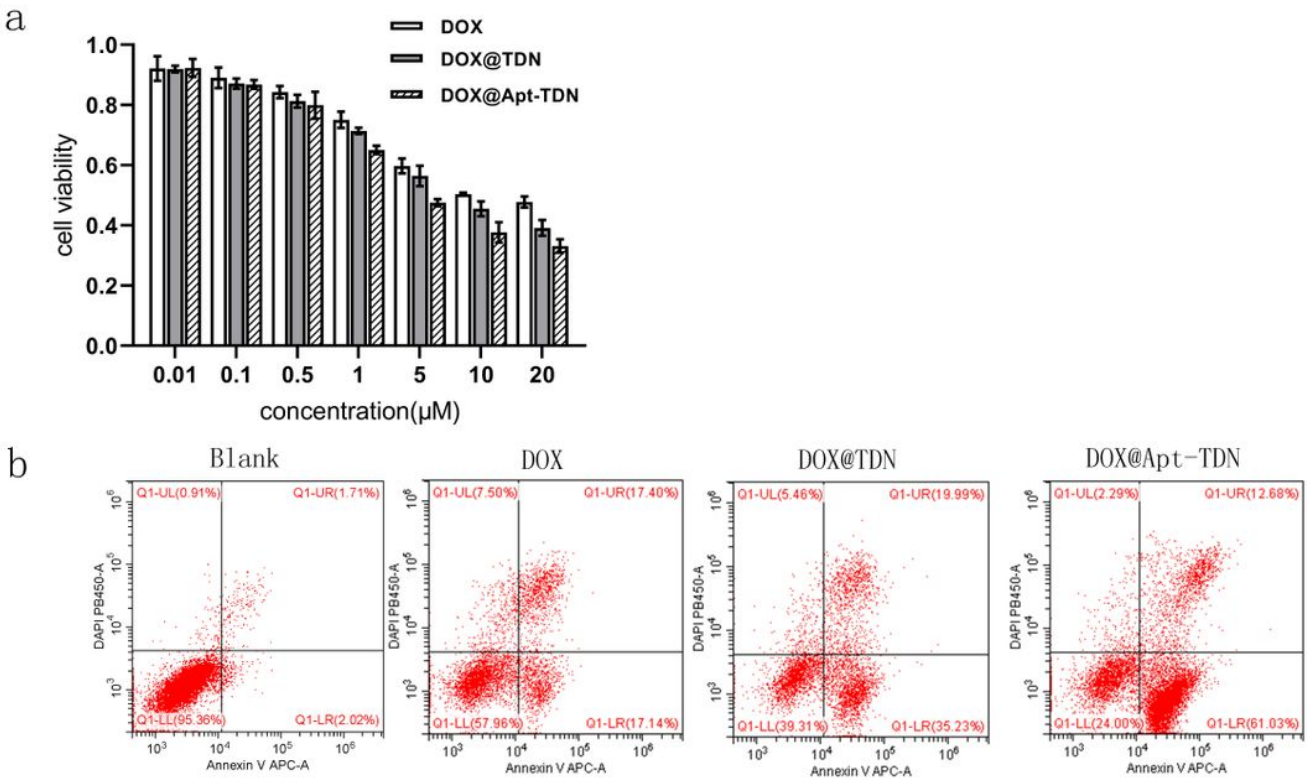

Figure 6

(a)Cyto toxicity of DOX, DOX@TDN, and DOX@ Apt TDN at various concentration s . The inhibition rate of the U87 cells increased significantly with increas ing of DOX concentration, but at the same concentration, the DOX@TDN and DOX@Apt TDN groups significantly increased cytotoxicity compared with the DOX group alone . T he cell inhibition rate of the DOX@Apt TDN group was also significantly h igher than that of the DOX@TDN group (p< b) Apoptotic statistics of U87MG cell after incubation w ith PBS, DOX, DOX@TDN, DOX@Apt TDN for 24 h . (Flow cytometry histograms of U87MG c ell cycle after incubation with PBS, DOX@TDN, DOX@Apt TDN for 24 h.